 DOI: 10.1002/masy.200900021

Fiber - and Tube - Formation by Melt Infiltration of Block Copolymers into Al_2O_3-Pores

Bhanuprathap Pulamagatta,[1] *Wolfgang H. Binder,**[1] *Eric Yau,*[2] *Ilja Gunkel,*[3] *Thomas Thurn-Albrecht,*[3] *Martin Steinhart*[2]

Summary: We report on the formation of polymer nanofibers and nanotubes by melt infiltration of block copolymers (BCPs) containing poly (norbornene) blocks bearing polar and non-polar moieties synthesized via ring opening metathesis polymerization (ROMP) into Al_2O_3 porous templates. The effect of pore size of the Al_2O_3 template and polymer chain length on the formed structure i.e. fibers or hallow tubes is investigated. SEM analysis revealed that a smaller pore size ($\sim$ 180 nm) of the Al_2O_3 template with a BCP of lower molecular weight ($<$ 15 kg/mol) results in complete filling of the pores to yield fibers in contrast to bigger pore size (400 nm) or higher molecular weights ($>$ 25 kg/mol) furnishing hollow tubes.

Keywords: block-copolymers; melt infiltration; nanofibers; nanotubes

Introduction

Arrays of aligned one-dimensional polymer nanostructures can be exploited as substrates for tissue engineering, drug delivery systems, surfaces with tailored wetting and adhesion properties as well as filters and sensor arrays. Wetting nanoporous hard templates such as anodic aluminum oxide (AAO) with polymer melts has been explored as a versatile access to assemblies of polymer nanotubes[1] or fibers.[2] Infiltration may involve the rapid formation of precursor films on the pore walls of the hard template[3] or the slow filling of the pore volume by a solid thread of the molten polymer driven by capillary forces. Thus, either nanotubes or fibers are obtained after solidification of the polymer. Steinhart and co-workers[1,4,5] as well as Zhang et al.[6] were successful in fabricating the nanotubes by wetting alumina membrane by homopolymer melts such as PS, PMMA and PTFE. However, up to now, infiltration of BCPs into AAO exclusively yielded solid nanofibers obtained by capillary wetting,[7–9] whereas infiltration of BCP solutions has suffered from the lack of controllability of processes involving the evaporation of volatile solvents. In this work we investigate the melt infiltration of functionalized norbornene-[10] and oxynorbornene-[11] based block-copolymers designated as BCP-A_mD_n as shown in Scheme 1, synthesizing norbornene block copolymer with different molecular weights and block composition via sequential ring opening metathesis polymerization (ROMP).

Experimental Part

Materials

All reagents were purchased from Sigma-Aldrich and used without further purification. Dichloromethane was freshly distilled over CaH_2 and degassed with argon prior to use.

Instrumentation

GPC analysis was done on a Viscotek VE2001 system. Polystyrene standards were

[1] Institute of Chemistry, Department of Macromolecular Chemistry, Martin-Luther-University Halle-Wittenberg, D-06099 Halle, Germany
E-mail: wolfgang.binder@chemie.uni-halle.de
[2] Max Planck Institute of Microstructure Physics, D-06120 Halle, Germany
[3] Institute of Physics, Martin-Luther-University Halle-Wittenberg, D-06099 Halle, Germany

Copyright © 2010 WILEY-VCH Verlag GmbH & Co. KGaA, Weinheim

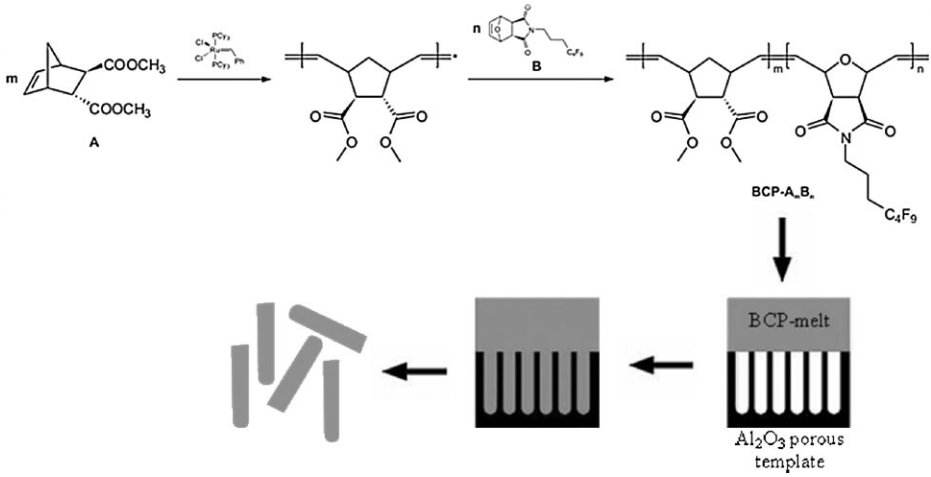

Scheme 1.
Synthetic pathway to prepare block-copolymer (BCP- A_mD_n) and melt infiltration process into a Al_2O_3 porous template.

used for conventional external calibration using a Viscotek VE3580 refractive index detector. DSC and TGA experiments were conducted on Mettler Toledo (DSC-H22) instrument under nitrogen atmosphere, heating rate 10 K/min, acquired Tg values were from second heating run. SAXS measurements on bulk samples were performed on JJ-Xray setup based on a 2D detector Brucker Hi-star installed on rotating anode from Rigaku. The SEM images were taken with JEOL JSM-6701F microscope.

Synthesis of endo,exo[2.2.1] bicyclo-2-ene-5,6-dicarboxylic acid dimethylester (monomer A). A modified literature synthesis[10] was adopted.

Synthesis of exo-*N*-(4,4,5,5,6,6,7,7,7-nonafluoroheptyl)-10-oxa-4-azatricyclodec-8-ene-3,5-dione (monomer D) was done according to the procedure given in reference.[11]The product was purified by chromatography (SiO_2, hexane/ethyl acetate =1/1) in order to yield white crystals of monomer D.

^{1}H NMR (δ ppm, 400 MHz, $CDCl_3$): 6.51 (td, $J = 4.42$, 0.80, 0.80 Hz, 2H), 5.26 (td, $J = 1.87$, 0.90, 0.90 Hz, 2H), 3.57 (t, $J = 6.92$, 6.92 Hz, 2H), 2.88-2.83 (m, 2H), 2.14-1.97 (m, 2H), 1.95-1.83 (m, 2H).

General Synthesis Procedure of Block Copolymer-AD (BCP-AD)

As example for BCP-$A_{100}D_{100}$, monomer A (66.2 mg, 0.32 mmol) in 1ml of CH_2Cl_2 was added to the initiator [Grubbs 1st generation, $RuCl_2(PCy_3)_2(CHPh)$] (2.59 mg, 0.003 mmol) dissolved in 1 ml of CH_2Cl_2. The polymerization carried out at RT for 4 h till all of monomer A was consumed. Monomer D (133.9 mg, 0.32 mmol) in 1 ml of CH_2Cl_2 was added to the above reaction mixture and stirred for 4 h at RT till all of monomer D was consumed. The polymerization was quenched by adding cold ethyl vinyl ether. Half of the solvent in the reaction mixture was evaporated and the polymer was precipitated into cold methanol. The methanol was decanted and the product was dried in a high vacuum pump overnight to yield 197 g (98%) of BCP-$A_{100}D_{100}$.

BCP Melt Infiltration

A ordered porous alumina template surface covered with small slices of BCP were placed on a hot plate at 150 °C and the BCP melt was spread over the alumina surface homogenously. The alumina template with BCP on the top surface was placed in a cylindrical furnace at 150 °C under argon atmosphere and pressure was applied on

Copyright © 2010 WILEY-VCH Verlag GmbH & Co. KGaA, Weinheim

the template surface with help of a cylindrical weight for 48 hrs. After removing the samples from the furnace, their surface was carefully cleaned with sharp blade and the template was cut in two or three different angles to view under SEM.

Results and Discussion

The BCP-$A_{100}D_{100}$, BCP-$A_{25}D_{25}$ and BCP-$A_{140}D_{60}$ was obtained by sequential copolymerization of two monomers i.e. monomer A was first polymerized using Grubbs 1st generation initiator and then monomer D was co-polymerized onto the living polymer-A chains. Before adding the second monomer the complete polymerization of monomer A was confirmed by TLC and GPC measurements, the second monomer was then added. The GPC and DSC data of investigated block co-polymers are listed in Table 1. All GPC curves show monomodal distribution and polydispersity indices of ~ 1.2 confirming the successful crossover reaction and the living nature of the ROMP reaction. The molecular weights of BCPs obtained from the GPC measurements are lower than the calculated molecular weights presumably due to a systematic error of calibration standard i.e. the measurements are calibrated with polystyrene standards which is a different polymer from investigated BCPs. ^{1}H NMR spectra integral values prove the expected block ratios.

SAXS measurements were conducted on bulk samples without any pretreatment or annealing to find the BCP bulk morphology and domain size. The scattering curves of BCPs are shown in the Figure 1. The higher order scattering peaks i.e. up to third order peak (q_3) are visible in the

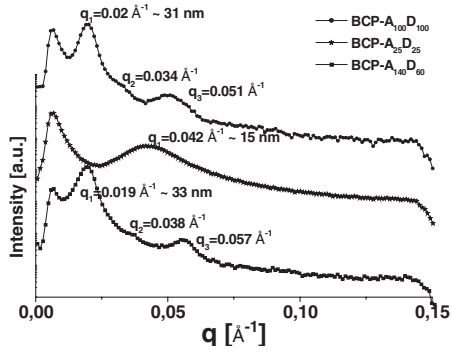

Figure 1.
SAXS of microphase separated BCP's-A_nD_n used for infiltration into nano-porous alumina membrane.

SAXS pattern, which indicates that the prepared BCPs have well ordered structures. In case of BCP-$A_{100}D_{100}$ a prominent first-order peak visible at $q_1 = 0.02$ $A^{\circ -1}$ and Second and third order peaks are positioned at $\sqrt{3}q_1$ and $\sqrt{7}q_1$ respectively, suggesting the hexagonally packed cylindrical morphology with the period of 31 nm. BCP-$A_{100}D_{100}$ have chain length ratio of 1:1, but in volume percent block-A accounts for only 33% and form cylinders in the matrix of block-D. Whereas the SAXS curves for BCP-$A_{140}D_{60}$ suggest the lamellar morphology with the period of 33 nm as q_2 and q_3 are $2q_1$ and $3q_1$ respectively (see Figure 1). The phase morphologies of prepared BCPs fit with classical BCP phase diagram. As the overall chain length decreases from 200 to 50 the broadening and lowering in the intensity of the peaks is observed with shifting of peaks to higher q values, means smaller phase domain size (see Figure 1 and Table 1). The higher order peaks are diminished in the case of BCP-$A_{25}D_{25}$ indicating a lower tendency of phase segregation due to the smaller block lengths.

Table 1.
GPC and morphological data of prepared block-copolymers.

Sample	$M_{n\ (cal)}$ (g/mol)	$M_{n\ (GPC)}$ (g/mol)	PDI	$Tg_{\ 1}$ (°C)	$Tg_{\ 2}$ (°C)	period (nm) $_{(SAXS)}$	morphology
BCP-$A_{140}D_{60}$	54 900	40 300	1.2	83.6	103.1	33	lamellar
BCP-$A_{100}D_{100}$	63 500	50 800	1.2	82.8	101.3	31	hexagonal
BCP-$A_{25}D_{25}$	15 875	14 200	1.1	80.1	—	15	—

Copyright © 2010 WILEY-VCH Verlag GmbH & Co. KGaA, Weinheim

BCP-$A_{100}D_{100}$ and BCP-$A_{25}D_{25}$ were melt infiltrated into 400 and 180 nm Al_2O_3 nanoporous membranes at 150 °C for 48 hrs. Figure 2a shows the SEM image of BCP-$A_{100}D_{100}$ melt infiltrated Al_2O_3 template with 180 nm pore size indicating a complete filling of the pores with BCP-$A_{100}D_{100}$,which upon etching away the Al_2O_3 with acid or base results nanofibers. Whereas in the case of 400 nm pore sized Al_2O_3 template BCP-$A_{100}D_{100}$ melt forms a precursor film on the pore walls by surface wetting mechanism to furnish hallow BCP nanotubes (see Figure 2d). Unlike BCP-$A_{100}D_{100}$, the BCP-$A_{25}D_{25}$ melt fills the 400 nm pores completely to form nanofibers (see Figure 2b and c). BCP-$A_{25}D_{25}$ with only 50 chain units has lower chain length i.e. lower molecular weight and viscosity as compared to BCP-$A_{100}D_{100}$ with 200 chain units, thus resulting in a different wetting behavior at the same temperature. This experimental observation clearly indicates that the formation of BCP nanotubes or nanofibers by melt infiltration of nanopore template wetting can be controlled by BCP chain length and template pore size.

Conclusion

We were able to synthesize functionalized norbornene block copolymers with lower PDI (~1.2) and controlled architecture via ROMP and successfully melt infiltrated these BCPs into Al_2O_3 porous template to obtain either nanofibers or nanotubes. Wetting behavior of the BCP melt depends on the polymer chain length and guides the formation of precursor film or completing filling of the high surface energy porous template. Alumina template of 180 nm pore size furnish nanofibers in contrast to hallow tubes formed with 400 nm template, hence the formation of fibers or tubes also depends on the pore size of the alumina template used for BCP infiltration. The prepared tubes serve as a potential platform for the production of functionalized polymer nanotubes.

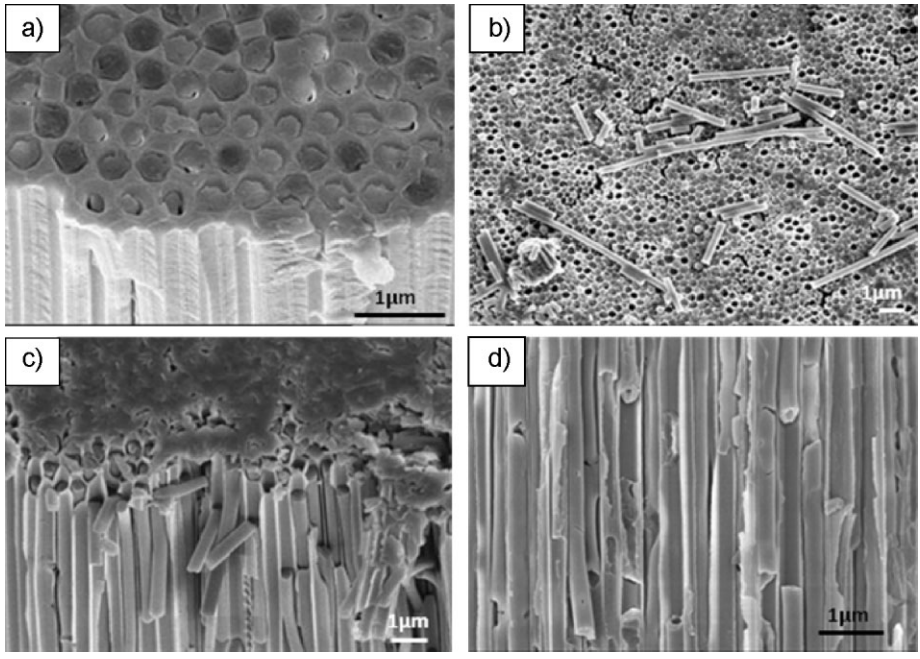

Figure 2.
SEM image of BCP melt infiltrated alumina templates a) top-view, BCP-$A_{100}D_{100}$ in 180 nm pore size. b, c) top view and side view BCP-$A_{25}B_{25}$ fibers in 400 nm pore size. d) Cross-sectional view along the 400 nm template where nanotubes of BCP-$A_{100}D_{100}$ are protruding out form alumina template.

Copyright © 2010 WILEY-VCH Verlag GmbH & Co. KGaA, Weinheim

[1] M. Steinhart, J. H. Wendorff, A. Greiner, R. B. Wehrspohn, K. Nielsch, J. Schilling, J. Choi, U. Gosele, *Science* **2002**, *296*, 1997–.
[2] K. Shin, H. Xiang, S. I. Moon, T. Kim, T. J. McCarthy, T. P. Russell, *Science* **2004**, *306*, 76–.
[3] M. Steinhart, R. B. Wehrspohn, U. Gösele, J. H. Wendorff, *Angew Chemie. Int. Edt.* **2004**, *43*, 1334–1344.
[4] O. Kriha, L. Zhao, E. Pippel, U.G.R., B. Wehrspohn, J. H. Wendorff, M. Steinhart, A. Greiner, *Adv. Funct. Mat.* **2007**, *17*, 1327–1332.
[5] M. Steinhart, S. M. A. , K. Schaper, T. Ogawa, M. Tsuji, U. Gösele, C. Weder, J. H. Wendorff, *Adv. Funct. Mat.* **2005**, *15*, 1656–1664.
[6] M. Zhang, P. Dobriyal, J. T. Chen, T. P. Russell, J. Olmo, A. Merry, *Nano Lett.* **2006**, *6*, 1075–1079.
[7] H. Xiang, K. Shin, T. Kim, S. I. Moon, T. J. McCarthy, T. P. Russell, *Macromolecules* **2004**, *37*, 5660–5664.
[8] Y. Wang, U. Goîšele, M. Steinhart, *Nano Lett.* **2008**, *8*, 3548–3553.
[9] W. Yong, Q. Yong, B. Andreas, Y. Eric, H. Changcheng, Z. Lianbing, G. Ulrich, K. Mato, S. Martin, *Adv. Mat.* **2009**, *9999*, NA.
[10] K. Stubenrauch, C. Moitzi, G. Fritz, O. Glatter, G. Trimmel, F. Stelzer, *Macromolecules* **2006**, *39*, 5865–5874.
[11] W. H. Binder, C. Kluger, *Macromolecules* **2004**, *37*, 9321–9330.

Copyright © 2010 WILEY-VCH Verlag GmbH & Co. KGaA, Weinheim